

Interaction between L-Tryptophan and Chlorogenic acid by using Molecular spectroscopy

A. Kanimozhi and S. Bakkialakshmi ^{a*}

Department of Physics,

Annamalai University, Annamalai Nagar,

Tamil Nadu, India

*Corresponding author email: bakkialakshmis@rocketmail.com

Abstract—The interaction between L-Tryptophan (L-TRP) and chlorogenic acid (CGA) was studied using UV/Vis absorption spectra, steady-state fluorescence, synchronous fluorescence spectra, Time-resolved fluorescence spectra, Fourier transform Infrared (FTIR), antibacterial activity, and molecular docking. The fluorescence of L-Tryptophan is exquisitely sensitive to the environment. It's sensitivity is related to luminescence properties originating from the hetero aromatic indole - ring of the residue with an uneven charge distribution around the macrocycle. Chlorogenic acid is the most abundant hydroxycinnamic acid naturally available in beverages of plant origin, such as coffee, and other agricultural product such as fruits, vegetables, cereals, and legumes. The conformation changes have been noted and the quenching mechanism between (L-TRP) and CGA proved to be static quenching by fluorescence. The binding constant and the number of the binding sites (L-TRP) on CGA were also calculated in this study.

Keywords: L-Tryptophan, Chlorogenic acid, Fluorescence, FTIR, Antibacterial activity, Anticancer activity and Molecular docking.

I. INTRODUCTION

L-Tryptophan (L-2-amino -3-(indole-3-yl)propionic acid) (L-TRP) is an essential amino acid that is required for the biosynthesis of proteins and is important in nitrogen balance and the maintenance of muscle mass and body weight in humans [1,2]. Tryptophan consists of D-tryptophan and L-tryptophan. D-tryptophan is hardly utilized by organisms [3]. L-tryptophan is one of the necessary amino acids for the life activities of creatures and is widely applied in medicine, food, and feedstuff investigating the interaction of drugs. For example, the interaction of L-tryptophan and p-hydroxyphenyl pyruvic acid or penicillin G with the fluorescence quenching method was studied [4, 5].

L-Tryptophan is a crucial part of protein synthesis. It serves as the precursor for various biomolecules. The tryptophan content shows a strong influence on some neurobehavioral effects, HIV infections, cancers, Alzheimer's, and Parkinson's disease [6,7]. Thus, the development of effective recognition methods for the sensing of tryptophan has been of intense interest. Detection of trace amounts of amino acids is quite important for disease diagnosis, food analysis, disease diagnosis, and for biomedical study.

These residues all contribute to absorption in the UV range [8,9]. However, the fluorescence spectra of most-tryptophan-containing proteins are dominated by tryptophan due to its high absorption extinction coefficient and efficient fluorescence [10]. They also perform as a precursor for synthesizing neurotransmitters in the human body, such as niacin, melatonin, and serotonin [11]. As an essential amino acid, TRP cannot be synthesized in the body. To keep enough TRP for balancing neurotransmitter levels, dietary TRP is required. Recommended daily TRP intake for adults is depending on the body weight [12]. L-Tryptophan is a natural amino acid that has both a fluorescent group and a binding unit, it has



been used in chiral recognition and has been shown to have a good fluorescence response. [13]. The structure of L-Trp has been shown in Fig 1.

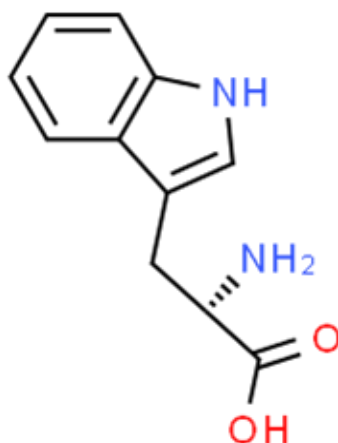


FIGURE 1: Molecular structure of L - Tryptophan

Polyphenols are a large class of secondary plant metabolites, widely distributed in the human diet such as fruit, vegetables, coffee, tea, chocolate, and beer [14]. Polyphenols have many biological activities, including powerful antioxidants which protect the body from damaging free radicals. [15]. Experimental and epidemiological evidence has demonstrated that increased intake of polyphenols is associated with a reduced risk of cardiovascular disease and cancer [16,17]. Thus, daily intake of polyphenols is important for human health. Chlorogenic acid (CGA) is the most frequent form of phenolic compound in plants. The presence of the phenolic group enables it to act as a natural antioxidant, and it can bind to enzymes and other multisubunit proteins, modify their structural properties and alter their biological activities [18]. CGA is present in green coffee beans and in citrus fruits, which are the best source of CGAs found in plants with an amount of 5 -12g/100g. The structure of Chlorogenic acid has been shown in Fig 2.

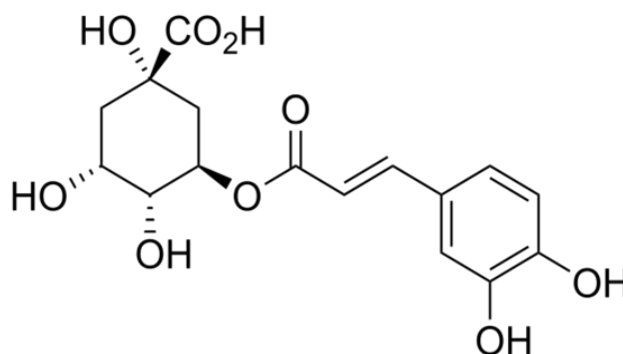


FIGURE 2: Molecular structure of Chlorogenic acid

Various studies have indicated that CGAs and their derivative have drawn the attention of many antioxidation [19,20,21], antimicrobes[22], antimutation, anticarcinogenic[23,24], antiviral[25], antihypercholesterolemia[26], antihypertensive[27,28] and Inflammatory actions [29]. Chlorogenic acids are also used in the regulation of blood sugar and have the potential to aid the management of obesity[30,31]. The risk of type-2 diabetes decreased with increasing coffee consumption in which the CGAs are responsible for anti-diabetic activity [32,33]. As is known to all, fluorescent methods have attracted enormous attention due to their good reproducibility, high sensitivity, excellent selectivity, non-destructiveness, and low cost. Recently, there are a variety of researchers who study the content of CGA, few groups use the fluorescence method to analyze the content of CGA.

CGA is widely distributed in many plants. As one of the most abundant polyphenols in people's daily diet, it is an important active ingredient in Chinese medicine [34]. Although the antioxidant properties of CGA are thought to reside in the catechol structure of the phenyl ring, the double bond conjugated with the catechol group may also serve as a site for free radical attack. Therefore, the stabilization of CGA is one of the most important concerns for its applications. It is a cinnamic acid of ester formed from caffeic acid and (-) - quinic acid [35].

The experimental studies, UV / Visible, Steady State fluorescence, Synchronous fluorescence, and time-resolved analysis assisted the conformation changes of L-Trp.

The influences of the polyphenols on the secondary structure of protein were studied by FTIR, Molecular Docking, and Antibacterial activity for the polyphenol, CGA have also been carried out.

II. MATERIALS AND METHODS

L-Tryptophan reagent grade ($\geq 98\%$) and chlorogenic acid ($\geq 95\%$) were purchased from Sigma-Aldrich Chemical Co. A stock solution L-Trp (10^{-4} M) was prepared with distilled water. The stock solution of chlorogenic acid (10^{-5} M) was prepared by using distilled water. The solutions were prepared just before taking absorption and fluorescence measurements

a) Spectroscopic instrument details

Absorption spectra were recorded between 200 to 400 nm with a SHIMADZU model (SHIMADZU 1800 PC UV/VIS spectrophotometer). Fluorescence spectra of each solution were recorded between 280 and 800 nm using an RF – 5301 PC (Shimadzu Corporation, Kyoto, Japan) fluorescence spectrophotometer. Fluorescence decay measurements were recorded using [Spectrofluorometer make Jobin Yvon model fluoro-log – FL3 – 11 spectrofluorometer]. FTIR spectra were recorded in a liquid sample of L-TRP with chlorogenic acid are measured from $4000\text{--}400\text{ cm}^{-1}$ [PerkinElmer model].

III. RESULTS AND DISCUSSION

a) UV –Visible spectroscopic study for L-TRP with chlorogenic acid

The UV/Vis absorption spectra of L-TRP and chlorogenic acid confirm the interaction mechanism. Interaction between amino acids and small biological molecules can be judged by changes in UV/Vis absorption spectra. The UV/Vis spectra of L-TRP with different concentrations of CGA [0, 0.2, 0.4, 0.6, 0.8, & 1.0 mol L⁻¹] are shown in Fig. 3. The absorption intensity of L-TRP at 280 nm increased with increasing ligand content, and certain redshifts were observed. The amino acid exhibited a strong characteristic absorption peak at around 280 nm which is attributed to the presence of L-Tryptophan. The maximum peak position of complexes red-shifted to 280, 283, and 289 nm for L-TRP and chlorogenic acid concentration [10^{-4} and 10^{-5} M]. In the absence of L-TRP, the UV/Vis absorption spectra of CGA are characterized by four absorption bands corresponding to HOMO → LUMO, mainly due to $\pi \rightarrow \pi^*$ orbital transition [36, 37]. With the gradual addition of CGA, the concurred and progressively enhanced peak at around 324 nm indicated the existence of binding interaction between L-tryptophan and CGA [38]. Besides, this confirms the binding interaction of L-Tryptophan with chlorogenic acid non-specifically and primarily by electrostatic mechanism [39].

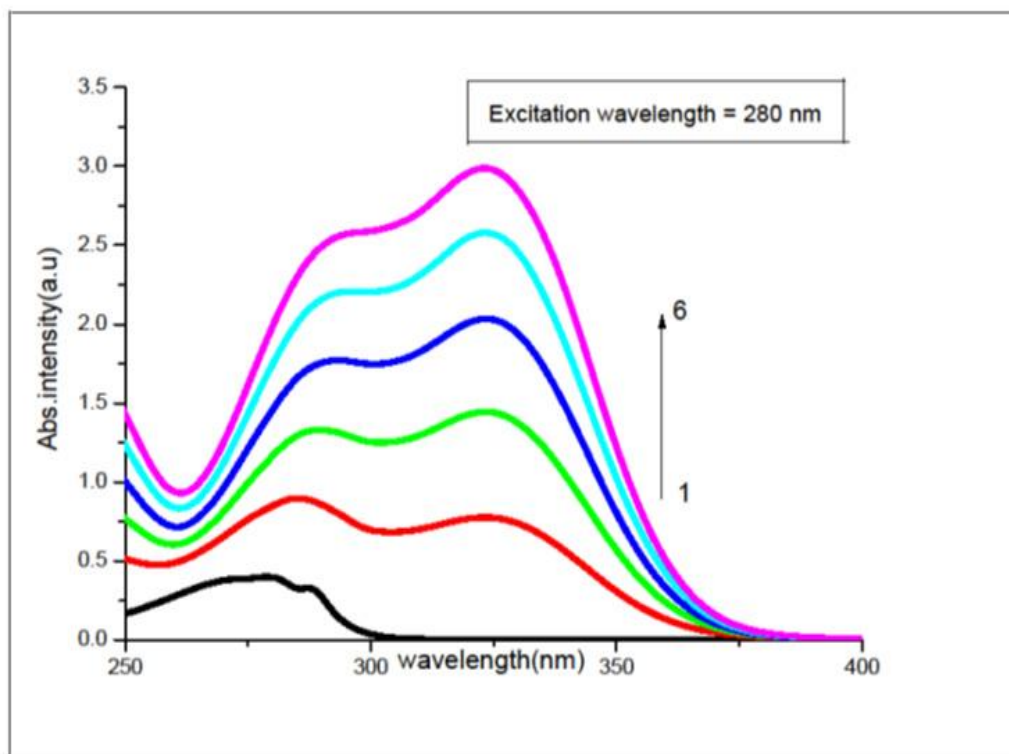


FIGURE 3: UV/Vis absorption spectra of L-Tryptophan with different concentrations of CGA (molL^{-1}) (1)0.0, (2)0.2,(3)0.4,(4)0.6,(5)0.8&(6)1.0

b) Fluorescence quenching mechanism of L-TRP by chlorogenic acid

Fluorescence quenching of L-TRP shows the change in fluorescence emission spectra with different concentrations of chlorogenic acid. The slit widths for the excitation and emission monochromators were set to 5 nm, respectively, and 600 scans were acquired per minute. The fluorescence maximum emission of Tryptophan (TRP) is sensitive to microenvironmentpolarity[40]From the spectrum, it was clear that the fluorescence intensity of L- TRP decreases at around 354 nm with increasing the concentration of chlorogenic acid. This is shown in Fig.4.

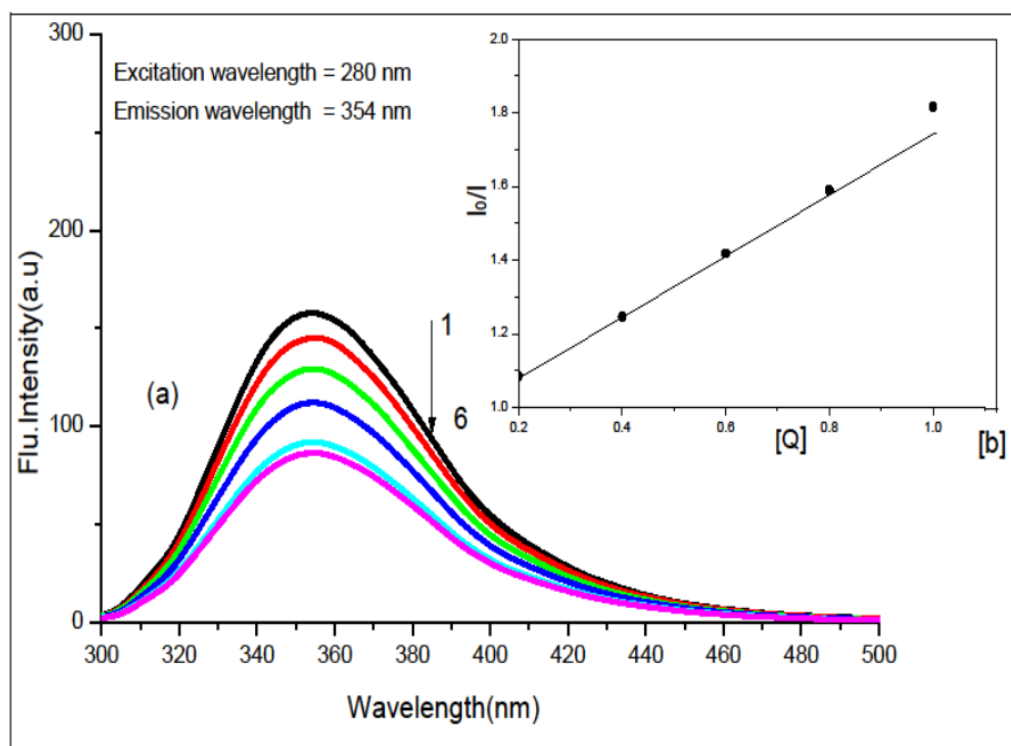


FIGURE 4. (a) Steady-state fluorescence spectra of L-tryptophan with different concentrations of chlorogenic acid (mol L^{-1}) (1) 0.0, (2) 0.2, (3) 0.4, (4) 0.6, (5) 0.8 & (6) 1.0. (b) Stern – Volmer plot of L-Tryptophan with chlorogenic acid

The fluorescence emission of L-TRP was quenched by chlorogenic acid with no spectral shift and indicating that interactions with chlorogenic acid do not influence the environment of fluorophores in amino acid. This suggested that the interaction of L-TRP with chlorogenic acid caused fluorescence quenching and changes in the microenvironment of the fluorophores. The fluorescence quenching can be divided into static quenching and dynamic quenching connected to the binding. For, dynamic and static quenching Stern- Volmer constant K_{SV} , an important parameter to distinguish the quenching mechanism, increases and decreases with the increase of concentration respectively. The following Stern- Volmer equation was used to calculate.

$$F_0 = 1 + K_{sv} [Q] = 1 + K_q \tau_0 [Q] \quad \text{----- (1)}$$

where F_0 and F denote the steady-state fluorescence (L-TRP) intensities in the absence and the presence of the quencher chlorogenic acid respectively. K_q is the biomolecular quenching rate constant, τ_0 is the average lifetime of the amino acid, $[Q]$ is the concentration of the quencher, and K_{sv} is the stern –Volmer quenching constant. The above equation is applied to determine K_{sv} by linear regression of a plot of (F_0/F) against $[Q]$.

The classical Stern – Volmer plot of L-TRP in the presence of CGA is shown in Fig 4. The stern-Volmer quenching constant and biomolecular quenching rate constant (K_q) are shown in Table 1.

Table 1 : Stern – Volmer (K_{sv}) and biomolecular quenching rate constant (K_q) of L-TRP with CGA

Quencher	$K_{SV} \times 10^{-5} (\text{L mol}^{-1})$	$K_q (\text{L mol}^{-1} \text{s}^{-1})$	R^a	S.D ^b
----------	---	---	-------	------------------

CGA	0.95	2.98×10^{13}	0.99	0.64
-----	------	-----------------------	------	------

^a→ is the correlation coefficient, ^b→ is the standard deviation

c) Synchronous fluorescence spectroscopy

The synchronous fluorescence spectra give information on the molecular microenvironment, particularly in the vicinity of the fluorophore functional groups [41]. When the wavelength intervals ($\Delta\lambda = \lambda_{em} - \lambda_{ex}$) are set at 15 nm and 60 nm, respectively. The effect of phenols on the conformational changes of L-TRP can be investigated by synchronous fluorescence spectroscopy. Synchronous fluorescence spectroscopy can be employed to analyze the conformational changes of amino acids and CGA. These spectra were used to detect the changes in the molecular microenvironment of the fluorophore functional groups. L-TRP combined with CGA were subjected to synchronous fluorescence to get additional information about the conformational changes present. Synchronous fluorescence spectra were recorded at for two $\Delta\lambda$ values (a) $\Delta\lambda = 15$ nm (b) $\Delta\lambda = 60$ nm. These are shown in Fig. 5.

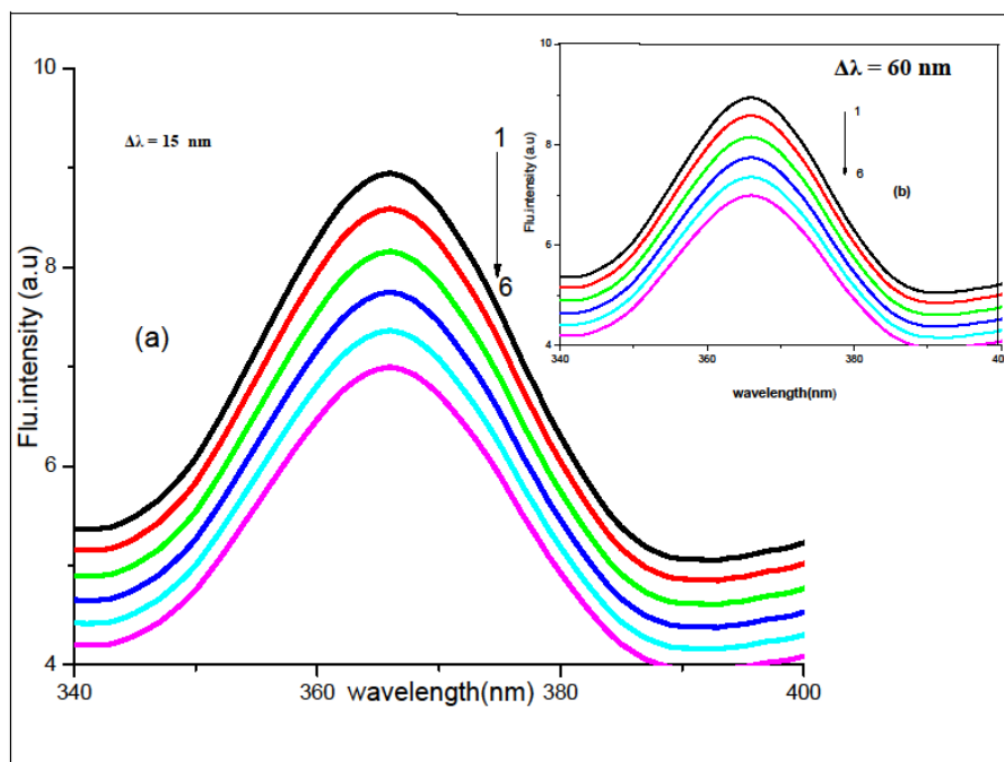


FIGURE 5: (a) Synchronous fluorescence spectra for L-Tryptophan with chlorogenic acid having (a) $\Delta\lambda = 15$ nm (b) $\Delta\lambda = 60$ nm

d) Binding constant and binding sites

Fluorescence quenching techniques can be used to determine the binding constant (K_a) and the number of binding sites (n) dependent on the interaction of L-TRP with CHL. Under the presumption that amino acids have independent binding sites. The values of K_a and n can be determined by using the formula, (equation 2)

$$\text{Log } (F_0 - F)/F = \text{log } K_a + n \text{ log } [Q] \quad \text{----- (2)}$$

The fluorescence intensities of the amino acid with and without the (CGA) quencher, are F and F_0 , respectively, and $[Q]$ is the initial quencher concentration Fig. 6. shows the double log plot L-TRP with CGA.

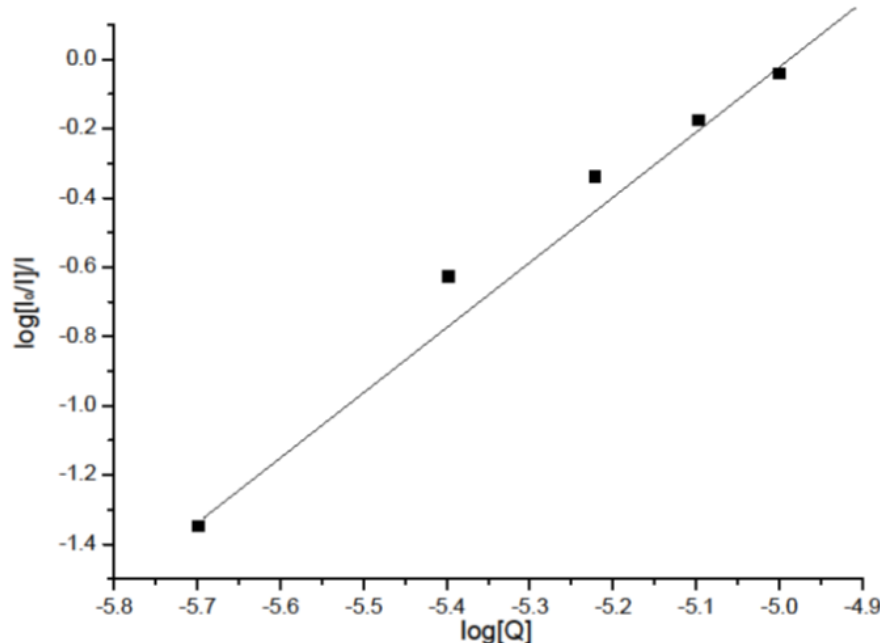


FIGURE 6: Double log plot of L-Tryptophan with chlorogenic acid

The K_a value of 1.51×10^6 was observed in Table 2. This Table 2 demonstrates that L-TRP and CGA had a strong binding interaction.

Table 2 : The binding constant (K_a), and binding site (n) correlation coefficient (R) of L-TRP with CGA.

Quencher	$K_a \times 10^6 (\text{Lmol}^{-1})$	n	R
Chlorogenic acid	1.51	0.91	0.94

e) Time-resolved fluorescence spectra for L-TRP with chlorogenic acid

Time-resolved fluorescence spectroscopy was applied to study the quenching mechanism. Fig. 7. Shows the fluorescence decay of L-TRP in the absence and presence of CGA. Fluorescence lifetime decay measurement provides one of the best parameters that help us to distinguish between the static and dynamic processes.

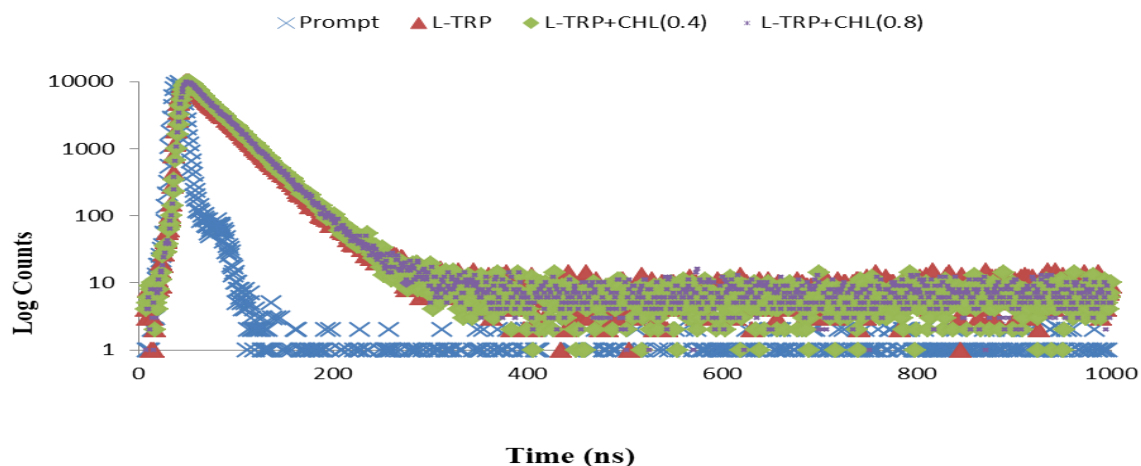


FIGURE 7: Time-resolved fluorescence spectra of L-Tryptophan with different concentrations of chlorogenic acid (mol dm^{-5}) (1) 0.0 (2) 0.4 and (3) 0.8

The fluorescence lifetime of L-TRP was learned in the absence and presence of chlorogenic acid. The average lifetime (τ) for biexponential interactive fittings was calculated from decay times and the relative amplitude (α) using the following equation (3)

$$\langle \tau \rangle = \frac{\tau_1 \alpha_1^2 + \tau_2 \alpha_2^2 + \tau_3 \alpha_3^2}{\tau_1 \alpha_1 + \tau_2 \alpha_2 + \tau_3 \alpha_3} \text{-----(3)}$$

The average fluorescence lifetime decrease from 3.20 ns to 3.05 ns without and with the chlorogenic acid, attesting that the fluorescence quenching here is fundamentally a static mechanism. The decay parameter for all the systems were summarised in Table 3. There is no obvious difference in the decay curves of L-TRP with the increasing amounts of Chlorogenic acid. For a static quenching the fluorescence lifetime of fluorophore will not disturb during the complex formation. Consequently a conclusion may be safely drawn that the quenching mechanisms of L-TRP by the CGA are all belongs to static quenching with complex formation. Table 3. Presents the fluorescence lifetime values of L-TRP without and with different concentrations of CGA. Thus, this observation shows that quenching follows static mechanism. These results are in good agreement with the results of steady state fluorescence

Table 3: Fluorescence lifetime and relative amplitudes of L-TRP with different concentrations of CGA

Concentration(M)	Lifetime(ns)			Averagelifetime $\times 10^{-9}$ sec	Relativeamplitude			χ^2	S.D $\times 10^{-11}$ sec		
	τ_1	τ_2	τ_3		B_1	B_2	B_3		T_1	T_2	T_3
L-TRP	3.18	5.72	4.23	3.20	88.28	6.49	5.23	1.27	9.11	3.95	5.59
L-TRP+CGA(0.4)	4.62	8.82	3.20	3.10	6.85	1.66	91.49	1.26	5.22	1.13	1.23
L-TRP+CGA(0.8)	1.22	3.31	3.81	3.05	3.10	91.22	5.67	1.27	1.60	1.65	7.63

f) Fluorescence Resonance Energy Transfer (FRET)

FRET is the physical process by which energy is transferred non-radiatively from an excited molecular chromophore (the donor D) to another chromophore (the acceptor A) using intermolecular long-range dipole-dipole coupling [42]. The overlap of UV absorption spectrum of CGA with fluorescence emission spectrum of L-TRP is shown in Fig. 8.

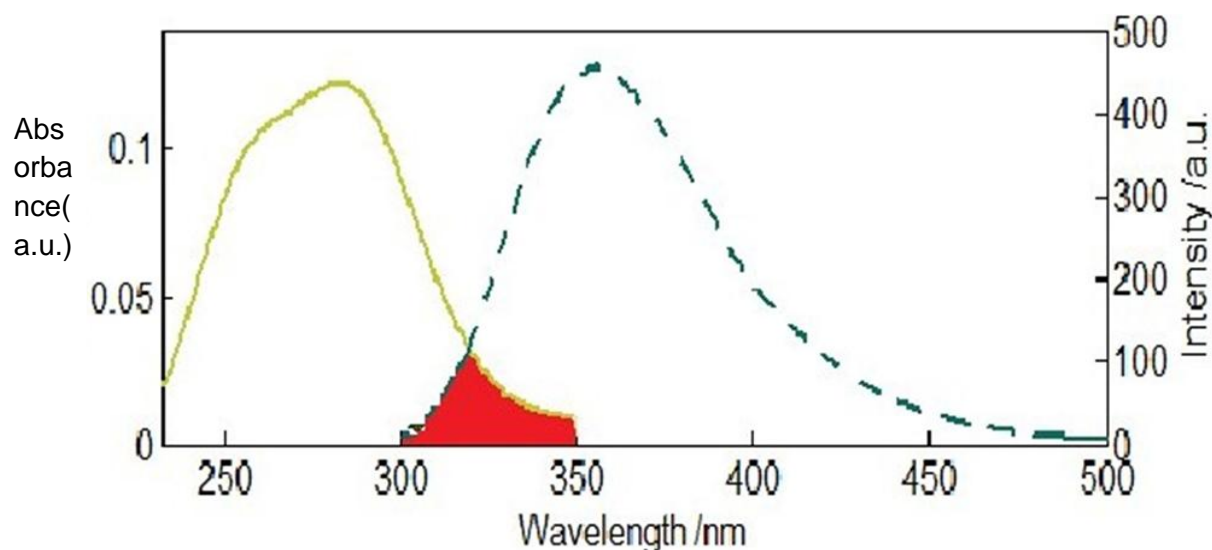


FIGURE 8: The overlap of UV absorption spectra of chlorogenic acid (solid line) with the fluorescence emission spectra of L-Tryptophan (dotted line)

The spectral studies suggested that interacted with L-TRP. The distance, r between the L-Tryptophan and the bound CGA could be determined using FRET. However, the r value calculated for CGA with L-TRP system is actually the average distance between the bound CGA. The efficiency of energy transfer, E , is calculated using the equation.

$$E = 1 - F/F_0 = R_0^6 / (R_0^6 + r^6) \text{----- (4)}$$

The fluorescence intensity of L-TRP with and without the acceptor is denoted by F and F_0 , Fig. 8. shows the overlap of UV absorption spectra of chlorogenic acid (solid line) with the fluorescence emission spectra of L-Tryptophan (dotted line). When the energy transfer efficiency is 50%, R_0 denotes the critical distance. The average distance between the donor and acceptor is denoted by r . The J is the overlap integral of fluorescence emission spectrum of donor and absorption spectrum of the acceptor [43, 44] was calculated using the overlapped component of the L-TRP emission spectrum and CGA absorption spectrum, and it was $5.20 \times 10^{-15} \text{ cm}^{-3} \text{ M}^{-1}$. Furthermore, the E , R_0 , and r values were 2.31 nm and 2.53 nm, respectively. Since the distance between L-TRP and CGA was 8 nm. The energy transfer from L-TRP with CGA exists with an immense probability.

g) FTIR spectroscopic study of L-TRP and CGA

FTIR spectroscopy is another technique for understanding conformations. The FTIR spectra of CGA and the physical mixture of L-TRP with CGA were recorded to conform to the complex formation. This is shown in Fig. 9.

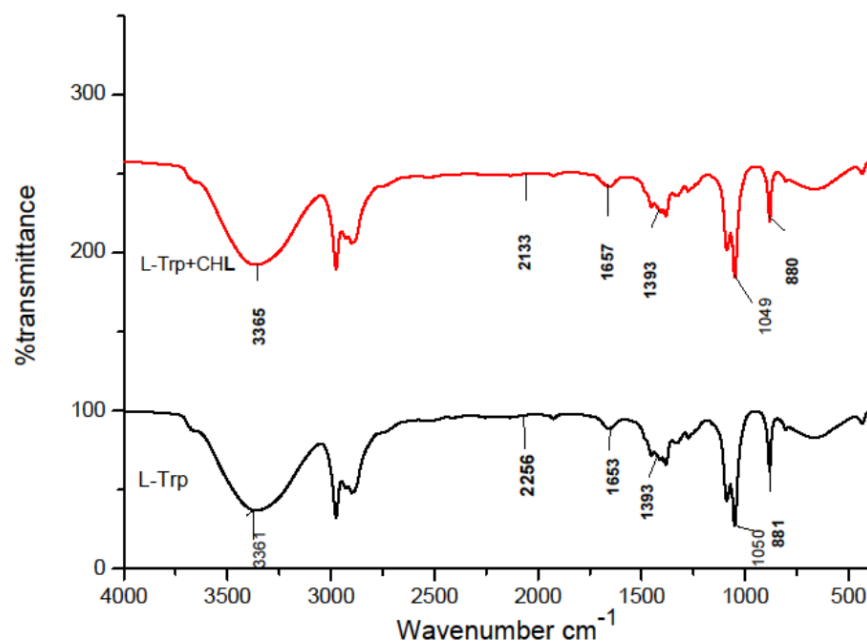


FIGURE 9: FTIR spectra of L-TRP+ CGA

All spectra were given an FTIR correction, and the area from 4000 to 400 cm^{-1} was chosen towards the path of the bands, with a peak suitable finished with the Opus software system[45]. Because of the complex interaction of atoms within the molecule, IR absorption of the functional groups may differ over a wide range of the FTIR bands at 4000 - 1450 cm^{-1} represents functional group region, the appearance of robust absorption bands in the region of 4000 to 2500 cm^{-1} was because of stretching vibrations between hydrogen and some additional atoms with a mass of 19 (or) less. The tentative peak assignment were given in Table.4.

Table 4: FTIR peak assignment of L-TRP without and with different concentrations of CGA

Wavenumber (cm^{-1})		Tentative Peakassignment
L-TRP	L-TRP+ CGA	
3361	3365	O – HStretching
2256	2133	C=CStretching
1653	1657	C-CStretching
1393	1382	C-NStretching
1050	1049	CO–O–COSTretching
881	880	C-HStretching

The spectra of L-tryptophan feature a broad and intensive band around 3400 cm^{-1} peak shift to 3361 cm^{-1} maybe due to the interaction of the chlorogenic acid with the OH band of L-tryptophan. The spectra of L-tryptophan 2256 cm^{-1} peak shifted to 2133 cm^{-1} C=C stretching. The spectra L-TRP 1653 cm^{-1} peak shifted to 1657 cm^{-1} C-C stretching. The spectra of L-TRP 1382 cm^{-1} peak shifted to 133 cm^{-1} C-N stretching. The

spectra of L-TRP 1050cm^{-1} peak shifted to 1049cm^{-1} CO–O–CO stretching. The spectra of L-TRP 881cm^{-1} peak shifted to 880cm^{-1} C-H stretching. This is shown in Table 4

h) Antibacterial activity

Both sensitive and resistant of gram-positive [staphylococcus aureus (S. aureus)] and gram-negative [Escherichia coli (E. coli)] were selected for antibacterial assay. The test organisms were staphylococcus aureus (s. aureus) ATCC (American Type Culture Collection) 25923, and Escherichia coli (E.coli) ATCC 25922. The qualitative antibacterial assay of the samples was carried out by the agar diffusion method [46, 47]. Bacteria have a great capacity for adjusting their metabolism in response to environmental changes by linking extracellular stimuli to the regulation of genes by transcription factors and in certain cases, transcription regulators control genes and operons that belong to different metabolic pathways. The bacterial pathogens were inoculated into the Muller Hinton broth and allow incubating for 24 hours at 37°C . The bacterial cultures were individually spread on the Muller Hinton agar plates and wells were made on 6mm by using a cork borer. The samples are dissolved in DMSO. Each well was loaded with $100\ \mu\text{l}$ of different samples and incubated at $28 \pm 2^{\circ}\text{C}$ for 24 h. The zone of inhibition was measured by the antibiotic zone scale. Finally, Antibacterial activity shows potent against both gram-positive and gram-negative bacteria. The antibacterial activity of L-TRP and chlorogenic acid using the Agar well diffusion method are shown in Fig. 10

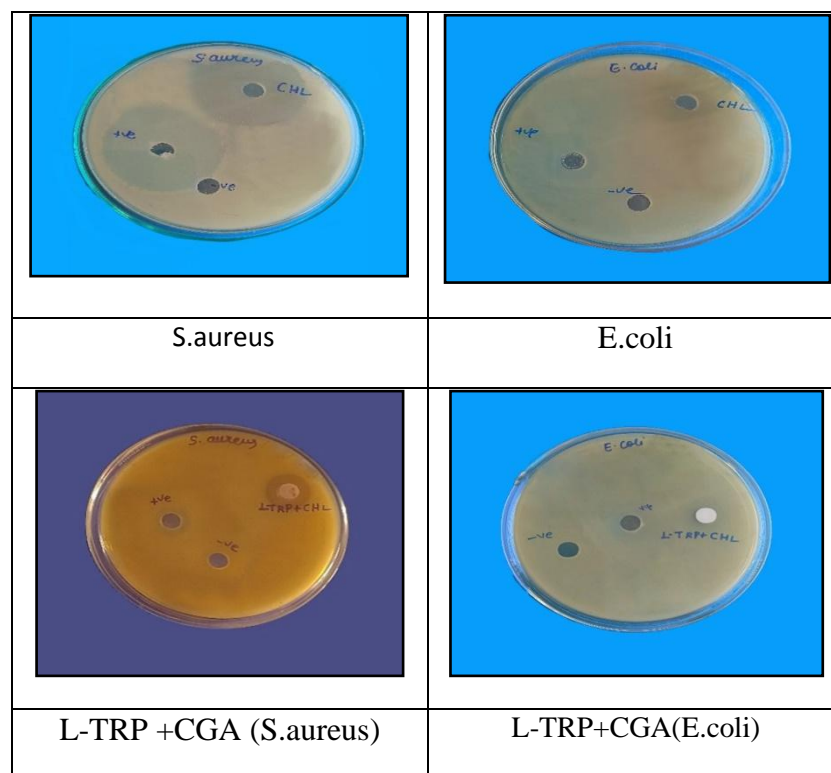


FIGURE 10: Antibacterial activity of L-TRP and Chlorogenic acid

As seen on the plates the sample had reacted to antibacterial activity. The zone of inhibition for the bacterial pathogens are tabulated in Table 5

Table 5: Antibacterial activity of L-TRP and Chlorogenic acid

s.no	Bacterial Pathogen	Zone Of Inhibition (mm)		
		L-TRP	CGA	L-TRP+CGA
1	S.aureus	10nm	21nm	20nm
2	E.coli	18nm	20nm	16nm

i) Anticancer activity of chlorogenic acid in cervical cancer cell line

Cervical cancer is characterized by the rapid and uncontrolled growth of abnormal cells on the cervix. The concentration of phytochemicals plays a role in their cytotoxicity and anticancer property. Probably, at higher concentrations, phytochemicals exhibit prooxidant properties and this pro-oxidant property might disrupt cellular activity. This might be the reason for the increased cytotoxicity at higher doses. The human cervical cancer cell line (HeLa) was plated separately using 96 well plates with a concentration of 1×10^4 cells/well in MEM media with 1X Antibiotic Antimycotic Solution and 10% fetal bovine serum (Himedia, India) in a CO₂ incubator at 37°C with 5% CO₂. The cells were washed with 200 µL of 1X PBS, then the cells were treated with various test concentrations of a sample (CGA) and with IC₅₀ concentration of Doxorubicin (12 µg/ml) as a positive control in serum-free media and incubated for 24 h. The medium was aspirated from cells at the end of the treatment period. 0.5mg/mL MTT prepared in 1X PBS was added and incubated at 37°C for 4 h using CO₂ incubator. After the incubation period, the medium containing MTT was discarded from the cells and washed using 200 µL of PBS. The formed crystals were dissolved with 100 µL of DMSO and thoroughly mixed. The development of color intensity was evaluated at 570nm. The formazan dye turns purple and blue color. The absorbance was measured at 570 nm using a microplate reader. The proliferation of HeLa cells was significantly inhibited by CGA in a concentration-dependent manner. The results of the anticancer activity test on chlorogenic acid in HeLa cervical cancer cells are presented in Fig .11 (a) &(b).

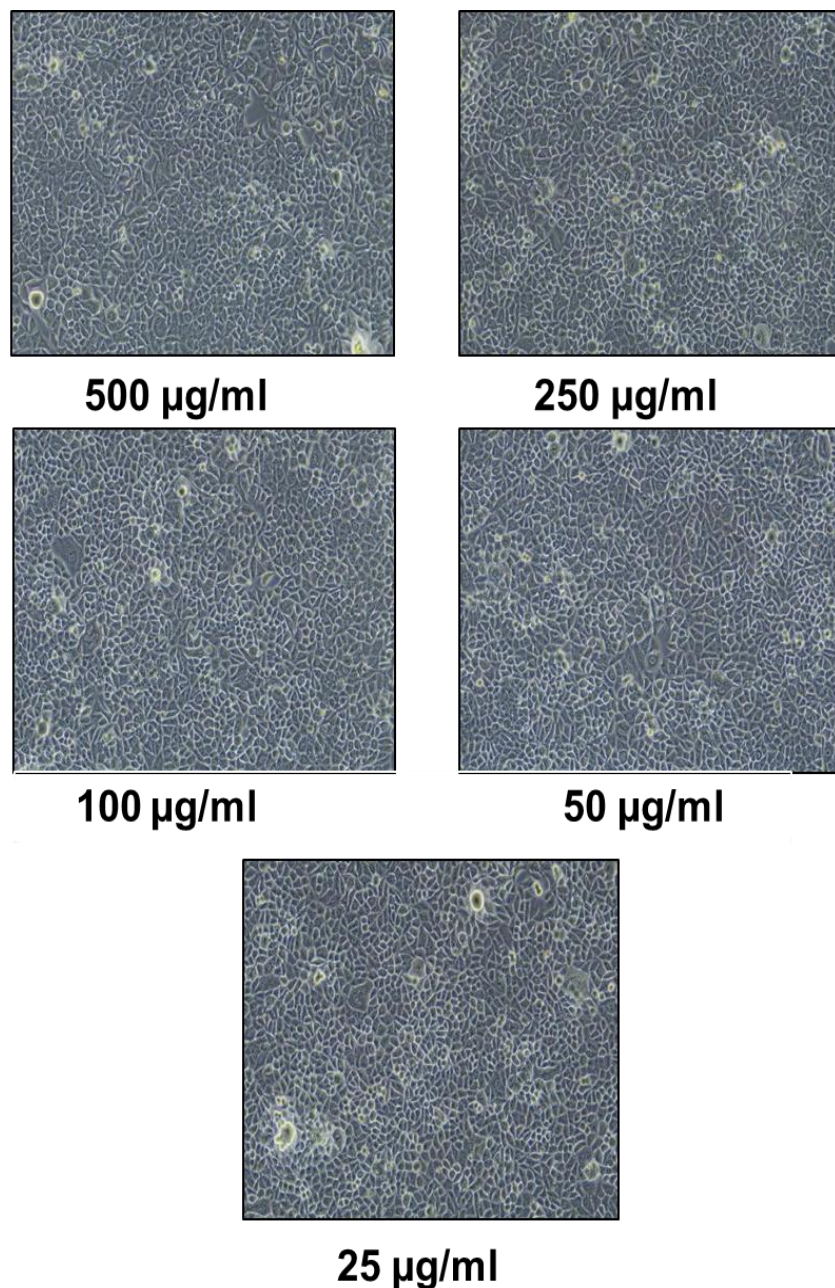


FIGURE 11:(a) & (b) Effect of chlorogenic acid different concentrations on cell viability microscopic image of HeLa cell.

The anticancer efficiency chlorogenic acid compound was human cervical cancer cell line (HeLa) and the effect of cytotoxicity on the cancer cell line was evaluated MTT assay method. The anticancer on the cervical cancer cell line was a different concentration of sample loading (25,50,100,250, and 500 µg/ml) shown in Fig.12. The graph shows that there is a positive relationship between the log concentration of the ethanol and extract and the percentage of inhibition of HeLa cervical cancer cells. It means that the higher the log concentration, the higher percentage of inhibition on HeLa cells. Therefore the largest concentration of inhibition, using 500 µg/ml.

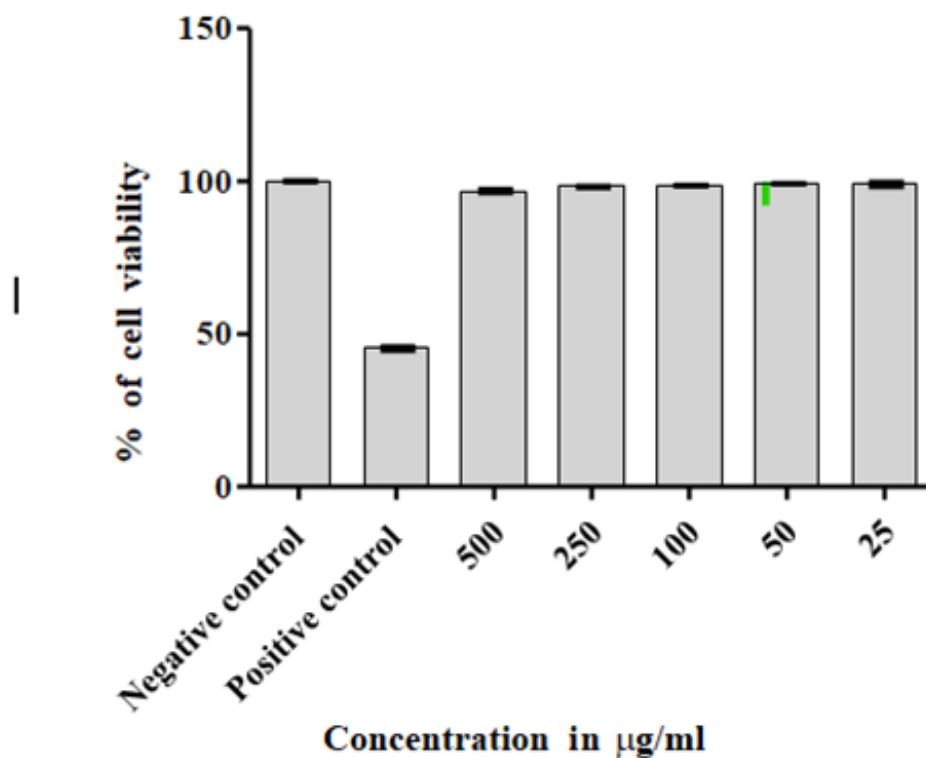


FIGURE 12:concentration versus cell viability

The anticancer activity of chlorogenic acid was exhibited by their anticancer effect on the HeLa cell line and the anticancer efficiency of the sample was expressed by IC_{50} value was The anticancer activity which is observed by the morphological image analysis is shown in Fig.13. $\text{IC}_{50} > 500 \mu\text{g/ml}$. Besides, while the concentration increases, the cytotoxicity increases leading to the death of cells and distinguished in a cervical cancer cell line.

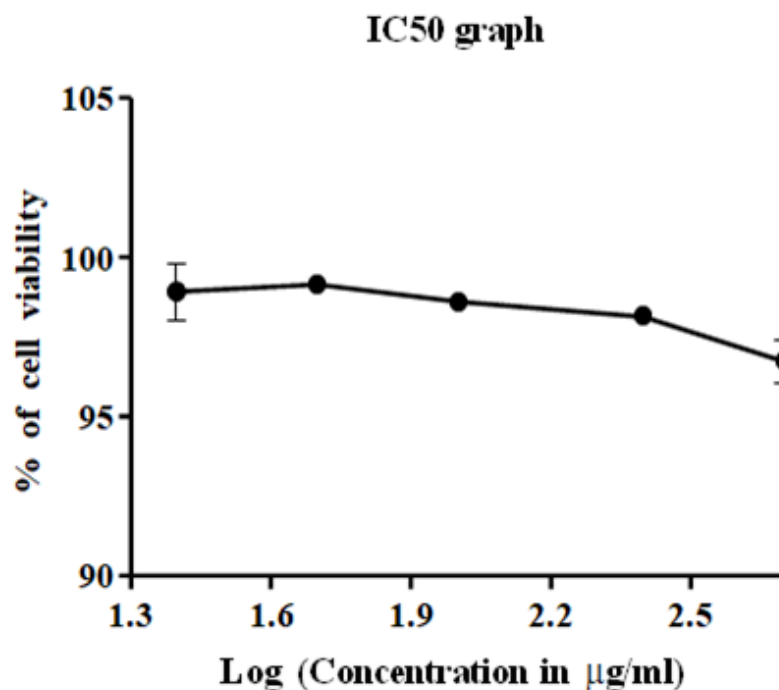


FIGURE 13: IC_{50} curve

Molecular docking is a well-organized approach that aids in the calculation of the ligand's leading binding modes and the structure of a three-dimensional protein. The ability to anticipate binding modes is critical for revealing significant structural properties and interaction, as well as providing helpful data in the development of effective inhibitors [48] that were used for docking studies. Molecular docking is one of the most widely used methods to predict the binding mode of a ligand into the binding pocket of a receptor. The structural data are stored in the Protein Data Bank (PDB) and freely available to the worldwide scientific community [49]. Auto dock vina software and auto dock tools were employed. Docking energy findings are shown in Fig .14(a) and (b.) S.aureus with CGA

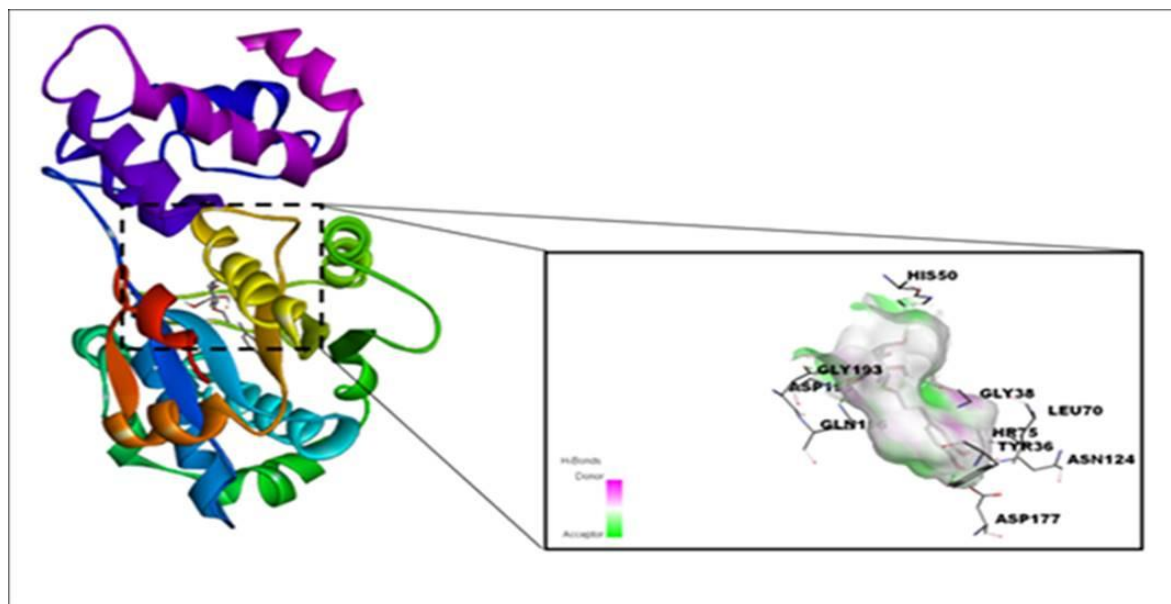


FIGURE (a)

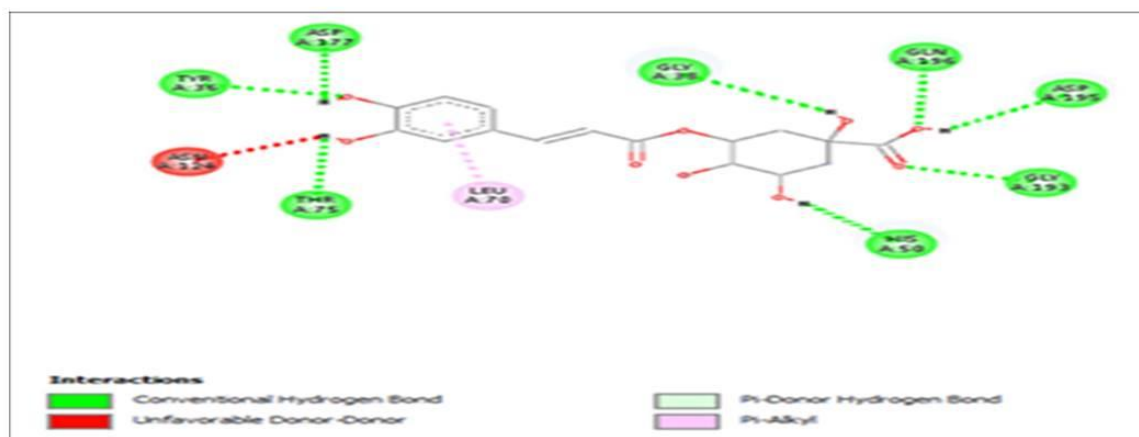


FIGURE (b)

FIGURE 14: (a) Docked complex of Tyrosyl-tRNA synthetase from *Staphylococcus aureus* (b) 2D Interaction Plot of Docked Complexes Tyrosyl-tRNA synthetase from *Staphylococcus aureus*

The Tryptophanyl-tRNA Synthetase from *Escherichia coli* and Tyrosyl-tRNA synthetase from *Staphylococcus aureus* protein targets were used in the molecular docking analysis. PubChem provided the three-dimensional structures of *S. aureus* with CGA and *E. coli* with CGA, whereas the protein data bank provided the crystal structures of *s. aureus* (PDB id: 1JIJ), and *E. coli* (PDB id: 5v0i)[50]. As a standard practice, the protein structure was prepared using the protein preparation wizard of the Auto dock before further use, which includes all water molecules in structures removed.[51]. Auto dock tools were used to add

hydrogen bonds and the hydrophobic (Amide – pi stacked). It can be found that variation between 1 and 2 Å for root mean square deviation (RMSD) values and a conserved binding pattern. The grid map points for s.aureus with CGA were 24 Å × 24 Å × 24 Å and e.coli with CGA were 35 Å × 24 Å × 24 Å. Here, the Lamarckian genetic algorithm (LGA) was used, the population size was about 150, and the maximum number of generations was about 27000. Docking results against s.aureus with CGA and e.coli with CGA, protein indicated a well-conserved binding region but with slightly predicted best binding energy values. Docking energy findings are shown in Fig. 15(a) and (b.) E.coli with CGA

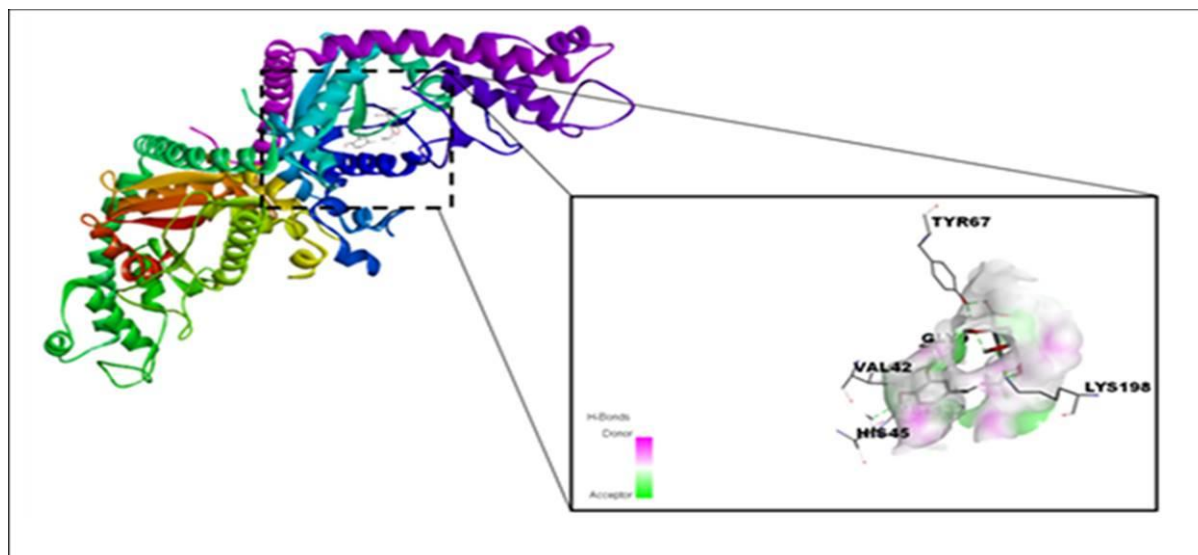


FIGURE (a)

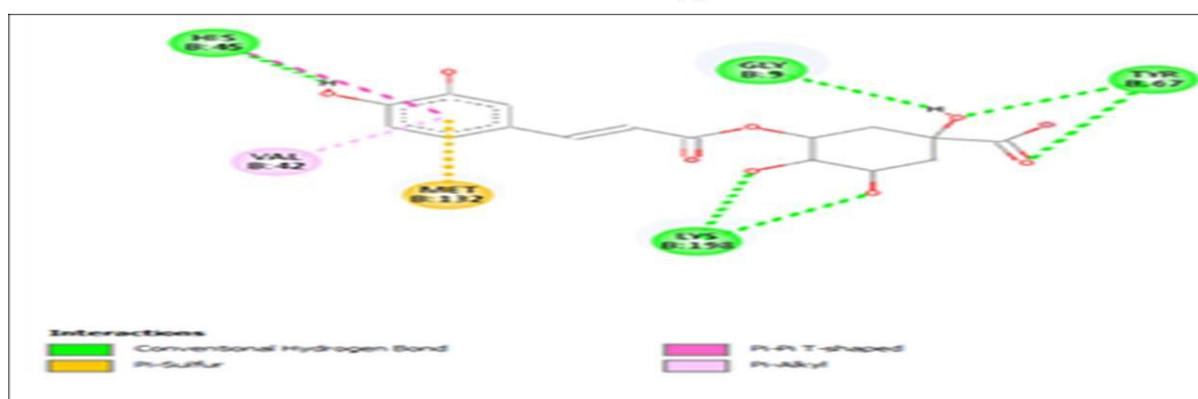


FIGURE (b)

FIGURE 15: (a) Docked complex of Tryptophanyl-tRNA synthetase from Escherichia coli (b) 2D Interaction Plot of Docked Complexes Tryptophanyl-tRNA synthetase from

The best free binding energy was found for compound S.aureus with CGA (−8.3 kcal/mol), and E.coli with CGA (−12.8 kcal/mol). Its interaction with Tyrosyl-tRNA Synthetase showcases 9 hydrogen bonds with the residues such as TYR A:36, GLY A:38, HIS A:50, LEU A:70, TYR A:75, ASN A:124, ASP A:177, GLY A:193, GLN A: and Tryptophanyl-tRNA synthetase showcases 5 hydrogen bonds with the residues such as GLY B:9, VAL B:42, HIS B:45, TYR B:67, MET B:132, LYS B:198 as shown in Table 6. The hydrogen bond between the active site residue of s.aureus with CGA and E.coli with CGA was also noted for interaction analysis. The structural stability of the binding modes is mainly due to the hydrogen bonds and also due to hydrophobic interactions between ligand–protein

components.

PDB code	Biological source	Protein name	RMSD Å	BindingEnergy ΔE (kcal/mol)
1JJJ	Staphylococcus aureus	Tyrosyl-tRNA synthetase (TyrRS)	3.2	-8.3
5V0I	Escherichia coli	Tryptophanyl-tRNA	1.90	-12.8

Table 6: Binding Energy ΔE (kcal/mol), and RMSD (Å) of S.aureus,E.coli with Chlorogenic acid

		Synthetase		
--	--	------------	--	--

IV. CONCLUSION

In this work, the specific interaction of L-Tryptophan with Chlorogenic acid was studied by various spectroscopic methods including Fluorescence spectroscopy, UV-Visible absorption spectroscopy, synchronous fluorescence spectroscopy, FTIR, antibacterial activity, anti-cancer activity and Molecular docking studies. The experimental results indicate that the quenching mechanism of fluorescence of L-TRP by chlorogenic acid is a static quenching process, the binding reaction is spontaneous, and electrostatic interaction played a major role in the reaction. From the spectra obtained, the quenching constants (K_{SV}), the binding constants (K_a), the number of binding sites (n), and the binding distance (r) are calculated. The hydrogen bond interaction might play a major role in binding chlorogenic acid to bacterial strains. Antibacterial activity results revealed the sample chlorogenic acid, a combination of L-TRP +CGA showed the maximum zone of inhibition against gram-positive [staphylococcus aureus (s.aureus)] compared with gram-negative [Escherichia coli(E.Coli)]. The further experiments at protein level are still needed to be performed for exploring this mechanism in detail which would further provide us another therapeutic approach for cervical cancer management. These results may provide a basis for the combined application of L-TRP and CGA in food and medicine.

Declaration of competing interest

The authors declare that they have no conflict of interests.

Funding

No funding was received for this work

Author contribution

A.Kanimozhi written the manuscript and Dr.S.Bakkialakshmi review the manuscript

Data Availability Statement

The authors confirm that all behavioral data to support the findings of our study are available in the paper.

References

1. A.M.Myint, Y.K.Kim,R.Verkerk,Kynurenine pathwayinmajordepression: evidence of impaired neuroprotection, *J. Affect. Disord.* 98 (2007)143–151.
2. A. Matin, I.M. Streete, I.M. Jamie, J.F. Jamie, A fluorescence-based assayforindoleamine 2,3-dioxygenase,*Anal.Biochem.*349(2006)96–102
3. Y.H. Hu, Y.H. Wang, H.S. Yu, et al., Advance of L-tryptophan applicationandproductiontechnology,*J.Jilin Agric.Univ.*30(2008)586–589
4. F.Y. Wu, M.G. Fu, X.S. Wei, et al., Fluorescence quenching method for thedeterminationofP-hydroxyphenylpyruvicacid,*Spectroscop.SpectralAnal.*21(2001)359–361.
5. R.S.Kumar,A.A.Prabhune,A.V.Pundle,etal.,Atryptophanresidueisidentified in the substrate binding of penicillin G acylase from *Kluyveracitrophila*,*Enzyme Microb.Technol.*40(5)(2007)1389– 1397.
6. B.Y. Silber, J.A.J. Schmitt, Effects of tryptophan loading on humancognition,mood,andsleep,*Neurosci.Biobehav.Rev.*34(2010)387–407

7. M. Kia, A. Islamnezhad, S. Shariati, P. Biparva, Preparation of voltammetric biosensor for tryptophan using multi-walled carbon nanotubes, *Korean J. Chem. Eng.* 28(2011) 2064.
8. C.N. Pace, F. Vajdos, L. Fee, G. Grimsley, T. Gray, How to measure and predict the molar absorption coefficient of a protein, *Protein Sci.* 4(1995) 2411–2423
9. H. Mach, D.B. Volkin, C.J. Burke, C.R. Middaugh, Ultraviolet absorption spectroscopy, in: B.A. Shirley (Ed.), *Methods in Molecular Biology*, vol. 40, Humana Press, Totowa, NJ, 1995, pp. 91–114.
10. J.W. Longworth, Excited states of proteins and nucleic acids, in: R.F. Steiner, I. Weinryb (Eds.), *Excited states of proteins and nucleic acids*, Plenum Press, New York, 1971, pp. 319–484 Chapter 6.
11. GM. Kapalka. Chapter 4—substances involved in neurotransmission. In: Kapalka GM, editor. *Nutritional and herbal therapies for children and adolescents*. San Diego: Academic Press; 2010. p. 71–99
12. LI. Arranz. Chapter 13—effects of obesity on function and quality of life in chronic pain. In: Watson RR, Zibadi S, editors. *Nutritional modulators of pain in the aging population*. Academic Press; 2017. p. 151–70.
13. N. Voyer, J. Lamothe, *Tetrahedron* 1995, 51, 9241–9284; b) C. D. Tran, J. H. Fendler, *J. Am. Chem. Soc.* 1980, 102, 2923–2928
14. He, Y.; Wang, Y. W.; Tang, L. F.; Liu, H.; Chen, W.; Zheng, Z. L.; Zou, G. L. Binding of puerarin to human serum albumin: a spectroscopic analysis and molecular docking. *Journal of Fluorescence* 2008, 18(2), 433–442.
15. M. Abbas, F. Saeed, FM. Anjum, et al. Natural polyphenols: an overview. *Int J Food Prop* 2017; 20:1689–99. 10.1080/10942912.2016.1220393 [[CrossRef](#)] [[Google Scholar](#)]
16. M. G. L. Hertog, E. J. M. Feskens, D. Kromhout, P. C. H. Hollman, M. B. Katan, Dietary antioxidant flavonoids and risk of coronary heart disease – the Zutphen elderly study. *Lancet* 1993, 342(8878), 1007–1011.
17. M. Serafini, M. F. Testa, D. Villano, M. Pecorari, K. van Wieren, E. Azzini, A. Brambilla, G. Maiani, Antioxidant activity of blueberry fruit is impaired by association with milk. *Free Radical Biology and Medicine* 2009, 46(6), 769–774.
18. K. M. Livingstone, J. A. Lovegrove, D. I. Givens, The impact of substituting SFA in dairy products with MUFA or PUFA on CVD risk: Evidence from human intervention studies. *Nutrition Research Reviews* 2012, 25(2), 193–206
19. V. N. Uversky, Natively unfolded proteins: A point where biology waits for physics. *Protein Science* 2002, 11(4), 739–756.
20. A. Svilaas, AK. Sakhi, LF. Andersen, T. Svilaas, EC. Ström, DR. Jr. Jacobs, et al. Intakes of antioxidants in coffee, wine, and vegetables are correlated with plasma carotenoids in humans. *J Nutr* 2004; 134:562–7
21. Y. Sato, S. Itagaki, T. Kurokawa, T. Ogura, M. Kobayashi, T. Hirano, et al. In vitro and in vivo antioxidant properties of chlorogenic acid and caffeic acid. *Int J Pharm* 2011; 403:136–8.
22. GS. Yukawa, Effects of coffee consumption on oxidative susceptibility of low-density lipoproteins and serum lipid level on humans. *J Biochem* 2004; 1:70–4
23. AA. Almeida, A. Farah, DAM. Silva, EA. Nunam, MBA. Gloria. Antibacterial activity of coffee extracts and selected coffee chemical compounds against enterobacteria. *J Agric Food Chem* 2006; 54:8738–43.
24. U-H. Jin, J-Y. Lee, S-K. Kang, J-K. Kim, W-H. Park, J-G. Kim, et al. A phenolic compound, 5-caffeoylquinic acid (chlorogenic acid), is a new type and strong matrix metalloproteinase-9 inhibitor: isolation and identification from methanol extract of *Euonymus alatus*. *Life Sci* 2005; 77:2760–9.
25. CA. Gomes, TG. Cruz, JL. Andrade, N. Milhazes, F. Borges, MPM. Marques. Anticancer activity of phenolic acids of natural or synthetic origin: a structure-activity study. *J Med Chem* 2003; 46:5395–401.

26. GF.Wang , LP.Shi, YD.Ren, QF. Liu, HF. Liu, RJ. Zhang, et al. Anti-hepatitis B virus activity of chlorogenic acid, quinic acid and caffeic acid in vivo and in vitro. *Antiviral Res* 2009; 83:186–90.
27. C-W. Wan, CN-Y.Wong, W-K.Pin, MH-Y.Wong, C-Y.Kwok, RY-K.Chan, et al. Chlorogenic acid exhibits cholesterol lowering and fatty liver attenuating properties by up-regulating the gene expression of PPAR- α in hypercholesterolemic rats induced with a high-cholesterol diet. *Phytother Res* 2013; 27:545–51.
28. KS. Bhullar, G. Lassalle-Claux, M. Touaibia, HP. Rupasinghe. Antihypertensive effect of caffeic acid and its analogs through dual reninangiotensin-aldosterone system inhibition. *Eur J Pharmacol* 2014; 730:125–32.
31. Kozuma K, Tsuchiya S, Kohori J, Hase T, Tokimitsu I. Antihypertensive effect of green coffee bean extracts on mildly hypertensive subjects. *Hypertens Res* 2005; 28:711–8.
29. MD. Santos, MC.Almeida , NP.Lopes, GEP.Souza. Evaluation of the antiinflammatory, analgesic and antipyretic activity of the natural polyphenol chlorogenic acid. *Biol Pharm Bull* 2006; 29:2236–40
30. EE.Agardh, S. Carlsson, A. Ahlbom, S.Efendic, V. Grill, N. Hammar, et al. Coffee consumption, type 2 diabetes and impaired glucose tolerance in Swedish men and women. *J Inter Med* 2004; 255:645–52.
31. MT.Abidoff. Effect of chlorogenic acid administration on postprandial blood glucose levels. *Moscow Center Clinical Report* 1999;161–4.
32. Agardh EE, Carlsson S, Ahlbom A, Efendic S, Grill V, Hammar N, et al. Coffee consumption, type 2 diabetes and impaired glucose tolerance in Swedish men and women. *J Inter Med* 2004; 255:645–52.
33. J. Tuomilehto, G. Hu, S. Bidel, J. Lindström, P. Jousilahti. Coffee consumption and risk of type 2 diabetes mellitus among middle-aged Finnish men and women. *J Am Med Assoc* 2004; 291:1213–9.
34. M. Ali, J. K. Keppler, T.Coenye, & K.Schwarz, (2018). Covalent whey protein-rosmarinic acid interactions: A comparison of alkaline and enzymatic modifications on physicochemical, antioxidative, and antibacterial properties. *Journal of Food Science*, 83(8), 2092–2100.
35. Y. Zhang, & Q. X. Zhong, Q. X. (2012). Binding between bixin and whey protein at pH 7.4 studied by spectroscopy and isothermal titration calorimetry. *Journal of Agricultural and Food Chemistry*, 60(7), 1880–1886
36. J-P. Cornard, C. Lapougue, L. Danglerre, C. Allet-Bodelot. Complexation of lead(II) by chlorogenic acid: experimental and theoretical study. *J Phys Chem A* 2008;112:12475–84.
37. J-P. Cornard, C. Lapougue. Absorption spectra of caffeic acid, caffeate and their 1:1 complex with Al(III): density functional theory and time-dependent density functional theory investigations. *J Phys Chem A* 2006;110:7159–66.)
38. Y.Q. Wang, H.M. Zhang, Q.H. Zhou, *Eur. J. Med. Chem.* 44 (2009) 2100–2105
39. P. O. Vardevanyan., A. P. Antonyan, M. A. Parsadanyan, M. A. Shahinyan, & M. S. Mikaelyan, (2019). Study of Methylene Blue Interaction with Human Serum Albumin. *Biophysical Reviews and Letters*, 14(01), 17–25. <https://doi.org/10.1142/S1793048019500012>
40. R. N Santos, & A. D Andricopulo,. (2013). Physics and its interfaces with medicinal chemistry and drug design. *Brazilian Journal of Physics*, 43, 268-280.
41. T. Förster. Energy transport and fluorescence [in German]. *Naturwissenschaften* 1946, 6:166-175
42. T. Förster. Fluorescence of organic compounds [in German]. *Gettingen: Vandenhoeck & Ruprecht*: 1951:312.
43. Y.C. Fan, S.L. Zhang, J.C. Kong, et al., Study on the interaction between anionic liquid and L-tryptophan by fluorescence spectroscopic technique, *J.Microchem.*99(2) (2011)439–43. S. Z. Grinter and X. Zou, “Challenges, applications, and recent

- advances of protein-ligand docking in structure-based drug design,” *Molecules*, vol. 19, no. 7, pp. 10150–10176, 2014
44. H.M.Berman, J.Westbrook, Z. Feng, G.Gilliland, T.N.Bhat, H.Weissig, I.N. Shindyalov I.N, P.E.Bourne. The Protein Data Bank. *Nucleic Acids Res.* 2000;28:235–242. doi: 10.1093/nar/28.1.235. [[PMC free article](#)] [[PubMed](#)] [[CrossRef](#)] [[Google Scholar](#)]
- 45.Y. E. L. L. A. R. E. D. D. Y. Challa, V.Senthil, & N. Jawahar, (2022). preparation and characterization of lipid-polymer-hybrid nano particles of anti-alzheimer’s drugs-a research. *European Chemical Bulletin*, 11(4), 31-40.
- 46.Z. Lou, H. Wang, S. Zhu, C. Ma, Z. Wang (2011) Antibacterial activity and mechanism of action of chlorogenic acid. *J Food Sci* 76(6):M398–M403
- 47.X. Su,. A.B. Howell, D.H. D’Souza. Antibacterial effects of plant-derived extracts on methicillin-resistant *Staphylococcus aureus*. *Foodborne Pathog. Dis.* **2012**, 9, 573–578.
- 48.Y.C. Fan, S.L. Zhang, J.C. Kong, et al., Study on the interaction between anionic liquid and L-tryptophan by fluorescence spectroscopic technique, *J.Microchem.*99(2) (2011)439–.43.S. Z. Grinter and X. Zou, “Challenges, applications, and recent advances of protein-ligand docking in structure-based drug design,” *Molecules*, vol. 19, no. 7, pp. 10150–10176, 2014
- 49.R. Itri, W. Caetano, L. R. Barbosa, & M. S. Baptista,. (2004). Effect of urea on bovine serum albumin in aqueous and reverse micelle environments investigated by small angle X-ray scattering, fluorescence and circular dichroism. *Brazilian journal of physics*, 34, 58-63
- 50.R. A Jeyaram, & C. A. Radha,. (2022). Investigation on the binding properties of N1 neuraminidase of H5N1 influenza virus in complex with fluorinated sialic acid analog compounds—a study by molecular docking and molecular dynamics simulations. *Brazilian Journal of Physics*, 52(1), 21.
- 51.V.Alagarsamy, M. T.Sulthana, , J.Shanmugam, P. S Sundar,B. Narendhar. V. R., Solomon, & S. Srujana, (2022). Identification Of Promising Phytochemical Inhibitors For Sars-Cov-2 From Rosa Centifolia By Insilico Docking Studies. *European Chemical Bulletin*, 11(9), 88-88.